chemosensors

MDPI

Article

Design of Peptide Ligand for Lactoferrin and Study of Its Binding Specificity

Tatiana Zimina [1,2,*], Nikita Sitkov [1,2,*], Vladimir Karasev [1,2], Yury Skorik [3,4], Alexey Kolobov [2,5], Alexander Kolobov [5], Nikolay Bunenkov [6] and Viktor Luchinin [1]

1 Department of Micro and Nanoelectronics, Saint Petersburg Electrotechnical University "LETI", 197022 Saint Petersburg, Russia
2 Centre for Digital Telecommunication Technologies, Saint Petersburg Electrotechnical University "LETI", 197022 Saint Petersburg, Russia
3 Almazov National Medical Research Centre, 197341 Saint Petersburg, Russia
4 Institute of Macromolecular Compounds, Russian Academy of Sciences, 199004 Saint Petersburg, Russia
5 Laboratory of Peptide Chemistry, Institute of Human Hygiene, Occupational Pathology and Ecology, 188663 Saint Petersburg, Russia
6 Department of Bone Marrow Transplantation, Raisa Gorbacheva Research Institute of Children Oncology, Hematology and Transplantation of Pavlov First Saint Petersburg State Medical University, 197022 Saint Petersburg, Russia
* Correspondence: tmzimina@gmail.com (T.Z.); sitkov93@yandex.ru (N.S.)

Abstract: The in silico modelling of peptides complementary to lactoferrin was carried out using the Protein 3D software package and replication of the natural bonding site between pneumococcal surface protein (PSP) and lactoferrin (LF). The modeling was based on analysis of the conjugated ion–hydrogen bond systems between these proteins (CIHBS). The oligopeptide EEVAPQAQAKIAE-LENQVHRLE was proposed via computer modelling and synthesized using the solid phase synthesis technique, purified, and analyzed with MS and HPLC methods to confirm >95% purity. The peptide was then studied by capillary electrophoresis (CE). The CE experiments demonstrated the split of peptide zone in the presence of LF, due to complex formation and subsequent mobility change of the system peptide-protein. The reference experiments with homomyeloperoxidase and myoglobin did not show binding with LETI-11.

Keywords: peptide aptamers; biosensors; lactoferrin; electrophoresis; ligands

Citation: Zimina, T.; Sitkov, N.; Karasev, V.; Skorik, Y.; Kolobov, A.; Kolobov, A.; Bunenkov, N.; Luchinin, V. Design of Peptide Ligand for Lactoferrin and Study of Its Binding Specificity. *Chemosensors* **2023**, *11*, 162. https://doi.org/10.3390/chemosensors11030162

Academic Editor: Xiaolong Yang

Received: 3 February 2023
Revised: 18 February 2023
Accepted: 24 February 2023
Published: 27 February 2023

1. Introduction

The development of multiparametric diagnostics of non-communicable diseases (NCD) is becoming increasingly actual [1,2]. In fact, the prevalence of such diseases has begun to exceed the level of pandemic virus diseases, such as influenza and COVID-19, while their diversity requires special, complex, multifunctional diagnostics with the participation of many specialists [3]. A promising approach towards solving this problem is the application of multiparametric biosensors for detection of protein diagnostic marker-arrays and development of computer expert systems on this basis [4–6].

The main problem of such a diagnostic approach is the achievement of the selective recognition and binding of target marker protein (TMP). Antibodies are widely used as bioselective elements for binding TMPs in biosensor systems since they are natural protein molecules with high specificity and affinity for the target proteins. Antibodies have a number of limitations, namely, low stability at high temperatures, limited service life, high production cost, and the complexity of their chemical modification to increase the sensitivity and selectivity of the method [7]. These limitations could be minimized by using aptamers—synthetic oligonucleotides or oligopeptides with spatial complementarity to a certain region of the TMPs [8–11].

Originally, aptamers were produced by in vitro directed selection from combinatorial libraries of oligonucleotides. Aptamer isolation technology is called SELEX (systematic evolution of ligands by exponential enrichment) and is a multistage process [12].

Peptide aptamers are oligopeptides (consisting of 10–30 amino acids) that form spatial structures with a high degree of affinity and specificity of attachment to the TMP molecule. Peptide aptamers have dissociation constants that are comparable to, and sometimes even better than, those of antibodies [13]. Therefore, they are extremely promising for the development of biosensors for the detection of protein structures.

The number and diversity of approaches to designing peptide aptamers are ever-growing and their capabilities are improving every year. Modern in vitro methods are based on the improvement of the SELEX technology and are generally very expensive and laborious [12,13]. Alternatives to these methods are approaches based on the in silico atomic-molecular design of peptide aptamers and the analysis of their interactions with target proteins. The main directions of these approaches are molecular docking and non-stationary dynamic modeling [14–16].

Molecular docking is performed by virtual docking of the ligand to the binding site of the target protein and its movement to determine the location and conformation that will be most beneficial for selective binding. Proteins can possess several binding sites, and the use of docking is also one of the methods for assessing the quality of binding of a peptide aptamer to a target protein [14]. Non-stationary dynamic modeling allows one to form a detailed course of the aptamer-protein binding process [17–19]. Based on these methods, various computational services have been developed to search for binding sites for peptide aptamers with target proteins, such as pepATTRACT, FlexPepDock, HADDOCK [14–16], PEP-SiteFinder, and others [17–19].

The Engineering Center for Microtechnology and Diagnostics (CMID) of St. Petersburg Electrotechnical University "LETI" has developed an approach for atomic and molecular modeling of protein structures based on the model of a protein molecular vector machine (MVM) and the concept of Conjugated Ionic-Hydrogen Bond Systems (CIHBS) [20–22].

It is known from electronics that the features of functional electronic devices are determined by the choice of charge transfer principles and architectonics, and design methods. In biomolecular systems, processes associated with the transfer of charges (electrons and protons) also occur. Supramolecular structures of biosystems are similar to hierarchically organized electronic devices of ultra-high complexity [23], and their structure and properties should also be related to the principles of charge transfer [24]. As part of the development of the problem of charge transfer in biomolecular structures, the concept of CIHBS was proposed, which acts as the basis for their construction, as well as charge transfer channels design. Hydrogen atoms are taken as inputs, and lone pairs of electrons are taken as outputs in such molecular models, where molecular valves, signal delay elements, and charge sources are distinguished. The main conditions for the implementation of the model of charge transfer along with the CIHBS are the symmetry and subunit structure.

The atomic-molecular design of the peptide aptamers in silico is realized based on spatial analysis of the areas of possible interaction between the ligand and the marker. For the visualization of protein structures, the Protein 3D software developed earlier was used [21]. The software makes it possible to predict the amino acid sequence for the synthesis of peptide aptamers with spatial complementarity to target proteins, based on the contact region of neighboring globular proteins. Using this program, peptide sequences have been earlier proposed for a number of proteins that can be used as bioselective elements in analytical microsystems [4,5,25].

Thus, the considered methods of atomic-molecular design of bioselective elements in silico make it possible to create highly specific peptide recognition elements that can be integrated into multimodal microanalytical systems capable of implementing express-multiparametric detection, thus increasing the performance of the clinical analysis.

At present time, many groups of proteins have been identified as markers of various diseases, such as cardiovascular, oncological, lung diseases, diabetes, pancreatitis, etc., and described in data banks [26–29]. Lactoferrin (LF) is one of the important targets for diagnosing acute inflammatory processes and infections [30,31]. The important role of LF in maintaining the oxidative balance of the body is also noted [32]. LF is present in neutrophil granules, which tend to degrade under ischemic stress, releasing LF as well as myeloperoxidase (MPO). Concentration of LF correlates with concentration of MPO, which in turn is the marker of poor outcome of organ transplantation. It has also been reported that LF has an important role in supporting physiologic homeostasis during development of various pathologies due to its immunomodulatory nature, explained by the ability to monitor the immune status of an organism and act accordingly [33]. The functional role of LF in physiological homeostasis of an organism during development of disease and associated pathology is described in detail in the review [34]. The review data confirm an importance of LF as a prognostic marker of acute disease, when it fulfills its anti-inflammatory roles via different cell receptors and activation of various cell signaling pathways [34]. These features particularly explain an interest for clinical monitoring of LF levels during surgery, transplantation, acute viral or bacterial infections, etc. [35]. Normally, LF content in blood is reported as 59–345 ng/mL, while in pathology it could be about 10–500 μg/mL [36,37]. With such a scatter of values in the human blood, the dynamics of changes in this parameter are usually monitored [34,35].

Analytical strategies for determination of LF are described in a recent review [36]. In clinical practice, immunoassays (radial immunodiffusion (RID), enzyme-linked immunosorbent assay (ELISA), instrumental methods (reversed-phase high performance liquid chromatography (RP-HPLC)), and capillary electrophoresis (CE) are usually used [36]. Microfluidic devices using various detection techniques (fluorescence-based biosensor, sensor based on oligonucleotide aptamers with conjugated FITC, electrochemical immunobiosensor) are described [36]. A label-free surface plasmon resonance (SPR) immunoassay was used for detecting LF from human milk in the range of up to 1000 ng/mL [36].

It is important to note that LF is observed in blood in oligomer forms and as various complexes, for example, myeloperoxidase-lactoferrin-ceruloplasmin (MPO-LF-CP) [33,38,39]. This tendency for forming protein associations outputs further questions regarding selective determination via spatial recognition. For example, in [33], the interaction between this complex and peptides obtained via proteolysis of ceruloplasmin (CP), in which the peptides displaced CP bound to LF, is described. Thus, the problem of interaction site geometry and special location in the complex needs to be analyzed. It will be completed below in Section 3 of this article.

As shown in recent reports for the detection of LF using biosensor systems, antibodies or oligonucleotide aptamers are most often used as a biorecognition elements [36,37]. Peptide aptamers can be comparable to them in selectivity, and their synthesis is much cheaper. Therefore, the search for a peptide sequence capable of selectively recognizing and binding LF, and subsequently being used for its rapid detection in a biosensor format seems to be an actual and important enough task. However, the ultimate goal of the effort is development and implementation of high dimension/density multiparametric miniature devise for realization of system diagnostics. The implementing of such diagnostic systems needs a number of additional problems to be solved as well, besides in silico modelling of complementary ligands (aptamers) for selective binding of target proteins. These include design of high dimension/density miniature devises, and development of affordable registration principles [40], which are in the agenda for future work.

Presented in this article are results of the development and testing of a peptide to bind to a protein of the acute phase of inflammation, which contributes to regulating the functions of immunocompetent cells—lactoferrin (LF) [36,37].

2. Materials and Methods

2.1. Peptide Modelling

The analysis of the spatial structure of globular marker proteins capable of forming oligomers was carried out using the Protein 3D software (ETU, St. Petersburg) [21]. This software is designed to visualize supramolecular structures (primarily proteins) presented in the Protein Data Bank in PDB format [26]. As one of the forms of representation of the structure (rendering), the program implements the conjugated ionic-hydrogen bonds systems (CIHBS). The software allows the selection of continuous CIHBS analysis. Using this program, complementary regions of the subunit contact area were identified, and their prospects were assessed for the formation of stable systems of CIHBS, enabling the amino acid sequences for the creation of aptamer peptides on their basis to be proposed. Where necessary, sequence optimization could be performed to exclude fluorescent amino acid side chains interfering with fluorescent detection [4]. Thus, as an additional criterion in the process of selecting protein fragments suitable for use as aptamer templates, the analysis of CIHBS in the selected structures was used.

The concept of CIHBS is described earlier in the most complete form in [22]. The essence of this concept consists of the following statements:

(1) Supramolecular biostructures are built on the basis of the principle of continuity of type systems:

$$\begin{array}{cc} \text{R} & \text{R} \\ | & | \\ \ldots\ \text{HQ}_1\text{-R} = \text{X}_1\ \ldots\ \text{Z}_1\ \ldots\ \text{HQ}_2\text{-R} = \text{X}_2\ \ldots\ \text{HQ}_2\text{-R} = \text{X}_2\ \ldots & \ldots\ \text{HQ}_n\text{-R} = \text{X}_n\ \ldots\ \text{Z}_m\ \ldots\ . \end{array} \quad (1)$$

where: R—Zi—simple and Qi–R = Xi—resonance groups, containing instead of R, Z, Q, X, atoms of organogenic elements (C, N, O, P, S).

(2) These systems are utilized in biostructures as channels for energy and charge transfer. Formation of CIHBS in the area of subunit contact considerably promotes it stabilization.

2.2. Peptide Synthesis

Synthesis of the peptide was carried out by solid state method, in situ, using synthesizer "Applied Biosystems 430A (Applied Biosystems, Waltham, MA, USA)" and Nα-Boc-protected amino acid derivatives. The following types of trifunctional derivatives of amino acids were used: Boc-(Mts)Arg-OH, Boc-(Dnp)-His-OH, Boc-(OBzl)-Glu-OH, Boc-(ClZ)-Lyz-OH, etc. The synthesis was carried out using 0.1 mM of corresponding aminoacyl polymers with initial capacity of 0.5–0.8 mM/g. The polymer was 1% copolymer of styrene-divinylbenzene. Deblocking was performed using trifluoroacetic acid (TFA) for 1 min, twice. Neutralization at first condensation was made by adding a threefold excess of diisopropylethylamine (DIPEA) directly into the reaction chamber at the stage of bonding of amino acid residue [41]. Secondary condensation was made after the washing of peptydil polymer with 10% solution of DIPEA in dimethylformamide. Addition of amino acid residues was carried out by the method of 1-hydroxibenzotriazole ethers, using 2–5 fold excess of reagents and ninhydrin and bromophenol tests for control over the completeness of the reaction.

On completion of the peptide chain growth process, the product was treated with DMF:EDT:DIPEA (7:2:1 v/v) for 30 min and washed with DMF and DCM. Then washed with TFA twice for 1 min, washed with DCM and DEE, removed from the reactor, and dried.

The separation of peptide from polymer and removing of the side protective groups was carried out using liquid HF according to Sn1/Sn2 mechanisms under the presence of scavengers. The isolated products were cleaned using semi-preparative reversed-phase HPLC (Waters Prep Nova-Pak HR C-18, 6 μ, 60 Å, 19 × 300 mm^2) under gradient of acetonitrile. Detection occurred at 220 nm. The isolated fraction was analyzed with MS and HPLC methods showing the purity of >95%.

The samples of proteins and synthesized peptide LETI-11 are described in Table 1. The model proteins, MPO and MB, were selected for the following reasons: MPO as a protein, as its content often correlates with LF content in blood, forming complexes with LF in blood, and which was isolated for us, specifically for this work, from human leukocytes, by our scientific partners at The Institute of Experimental Medicine RAS; MB was selected as an iron-binding protein, which can be present in blood as a marker of myocardial infarction, and of appropriate *pI* and MW values. BSA could be a candidate, but its *pI* value was too close to LETI-11, which was not convenient for electrokinetic experiments.

Table 1. Proteins and peptide investigated and their properties.

No.	Sample	MW, Da	*pI*	Reference
1	Myoglobin from equine heart (MB); (Sigma-Aldrich, St. Louis, MO, USA)	117,199	6.8	[42,43]
2	Myeloperoxidase from human leucocytes in monomeric form (homoMPO); (IEM RAS, St. Petersburg, Russia)	75,000	5.62	[44–46]
3	Lactoferrin from human milk (LF) (IEM RAS, St. Petersburg)	80,000	8–9	[47–49]
4	Peptide (LETI-11): EEVAQAQAKIAELENQVHRLE (SPB ETU—IOPHS, St. Petersburg)	2345	5.6	[50]

2.3. Capillary Electrophoresis

The measurements were carried out using a Capel 105M capillary electrophoresis system (Lumex, Russia) [51] equipped with quartz capillaries with an internal diameter of 75 μm, a total capillary length of 60 cm, and the effective length of 50 cm. The experiments were carried out at temperature of 30 °C. The registration of the zones of the studied substances was carried out using a spectrophotometric detector at a wavelength of 200 nm. The wavelength was chosen due to the high level of absorbance of the peptide at the range of 200–220 nm [52,53].

Capillaries were prepared in two ways—A and B. Preparation of the capillary A procedure: washed with a solution of 1M HCl for 10 min, washing with deionized water for 10 min. Preparation of capillary B procedure: washing with deionized water for 5 min, washing with a solution of 1M HCl for 10 min, washing with deionized water for 10 min, washing with 0.5 M NaOH solution for 15 min, and finally washing with deionized water for 10 min. The capillaries were treated before every run.

The proteins and peptide were dissolved in 0.01 M Tris-HCl buffer solution with pH 7.2. The selection of chemical composition and pH of the buffer solution was determined by the goal of approaching native conditions for proteins.

3. Results and Discussion

3.1. Modelling of Peptide Ligand for Lactoferrin

Lactoferrin (LF) is a polyfunctional protein from the transferrin family [33,47–49,54]. It is a globular glycoprotein, and the human form contains 691 amino acids (AA). It consists of two domains linked by a covalent bond (analogues of the subunit). As shown in Figure 1, LF contains both α-helical regions (red fragments) and β-folds regions (green fragments).

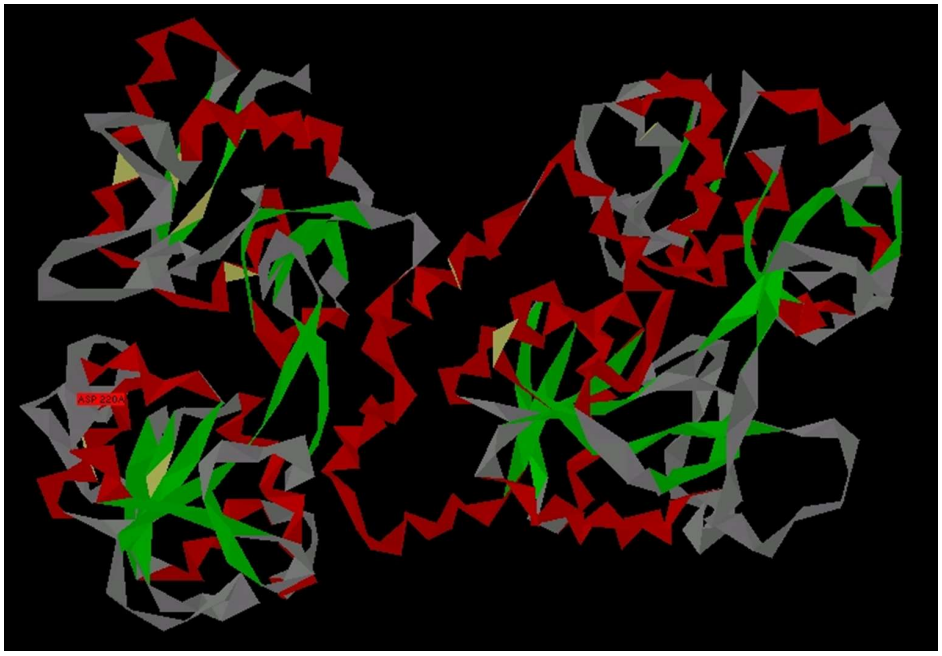

Figure 1. General view of human LF as a paper model (file 1B0L at PDB) obtained by rendering using Protein 3D software. α-Spiral parts (red); β-structures (green); left (N-lobe); and right (C-lobe).

LF is widely present in various secretory fluids such as milk, saliva, tears, and nasal secretions, as well as in blood. This protein is one of the components of the body's immune system, takes part in the system of nonspecific humoral immunity, regulates the functions of immunocompetent cells, and is an acute phase protein of inflammation. LF interacts with DNA and RNA, polysaccharides, heparin, and exhibits some of its biological functions in the form of complexes with these ligands.

However, for the purposes of this work, i.e., creating ligands that provide quantitative determination of this protein in tissues and biological fluids, these complexes are not very suitable, since they can also form complexes with other biomolecules.

Numerous structures of this protein are known, studied by X-ray diffraction analysis (XRD), some of which are presented in RSCB Protein Data Bank [26]. In our previous studies [4,25], we applied an approach that uses two principles: complementarity of the subunit contact area (to create ligands, amino acid sequences from the subunit contact area were used) and formation of systems of conjugated ionic-hydrogen bonds (CIHBS) to select optimal areas in the contact area. However, in the case of LF, the first principle does not work, since both parts of the protein are linked by a covalent bond and the formation of a complex with a ligand from the subunit contact area is impossible. For this reason, it was necessary to look for other complexes in which the patterns of protein-protein recognition are manifested.

One of the possible options used in this work is the formation of the LF complex with microbial proteins. For example, a complex described in [49] in which the LF complex with pneumococcal surface protein (PSP) was obtained. The authors of this work consider the formation of this complex, 2PMS, as an example of the manifestation of the immune antimicrobial properties of LF [26,49].

The entire protein was not used as a model, only the N-lobe of LF was used. The resulting complex, which crystallizes as a dimer, was examined by X-ray diffraction analysis with a resolution of 2.9 Å. This, of course, is not a very strong resolution, but when comparing the two subunits of the complex with other structures, as well as with the primary structures of homologous proteins, this complex was taken as the basis for the development of the ligand. As before, we used the Protein 3D software package [21].

As shown in Figure 2, the PSP molecule consists of three α-helical fragments, and not all of it participates in the formation of the complex, rather only one fragment participates.

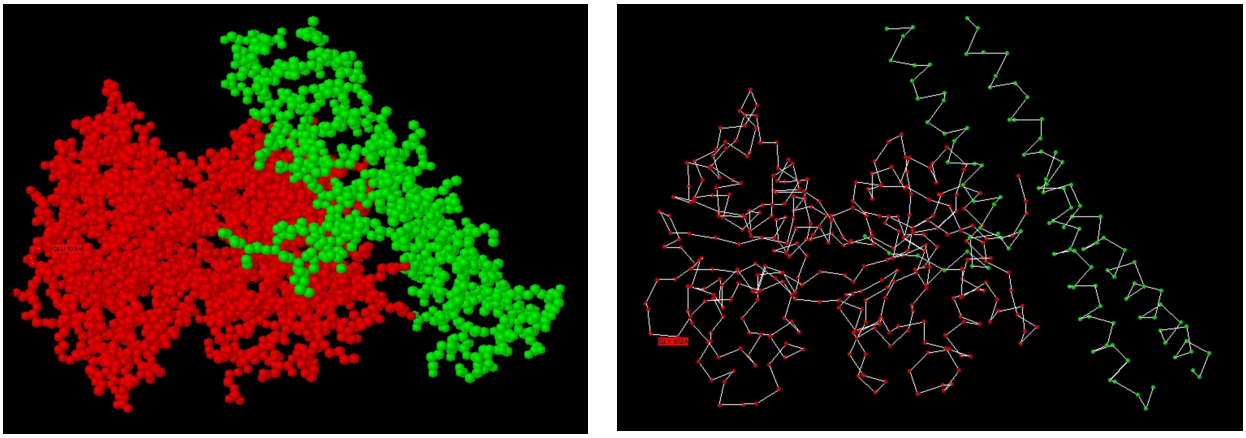

(**a**) (**b**)

Figure 2. General view of complex of N-lobe of LF (red) with pneumococcus surface protein (PSP—green) by rendering atoms (**a**); complex of N-lobe of LF with PSP by rendering CA-skeleton (**b**).

For the purposes of a more detailed analysis, we have reduced the number of amino acids in the file output by Protein 3D down to 60 amino acids in LF and to 20 amino acids in PSP. At the same time, it is possible to compare the A–C and B–D complexes (Figure 3a,b). Figure 3 shows that both variants are close in structure, although an identical arrangement cannot be obtained.

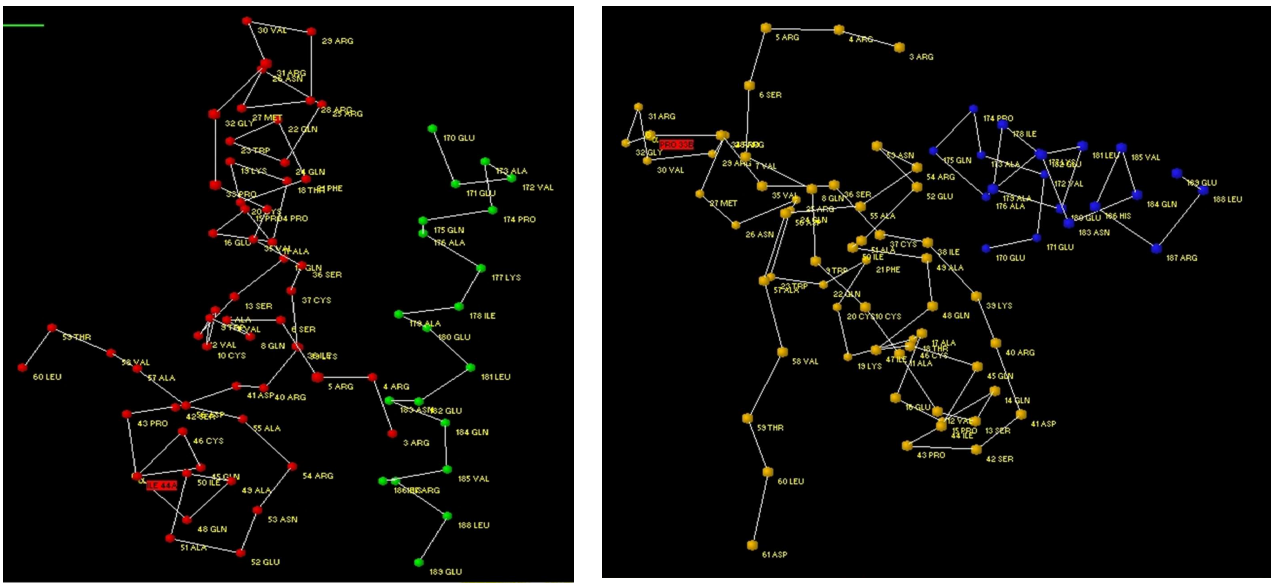

(**a**) (**b**)

Figure 3. Fragments of LF–PSP complex used for analysis: complex between A (red) and C (green) subunits (**a**), complex between B (yellow) and D (blue) subunits (**b**).

Further analysis was carried out separately for each of the two variants using CIHBS. Figure 4 shows CIHBS during the formation of hydrogen bonds between His 186, Glu 182 of PSP and Gln 45, Arg 40 of LF. It is easy to verify that the composition obtained for both variants is identical.

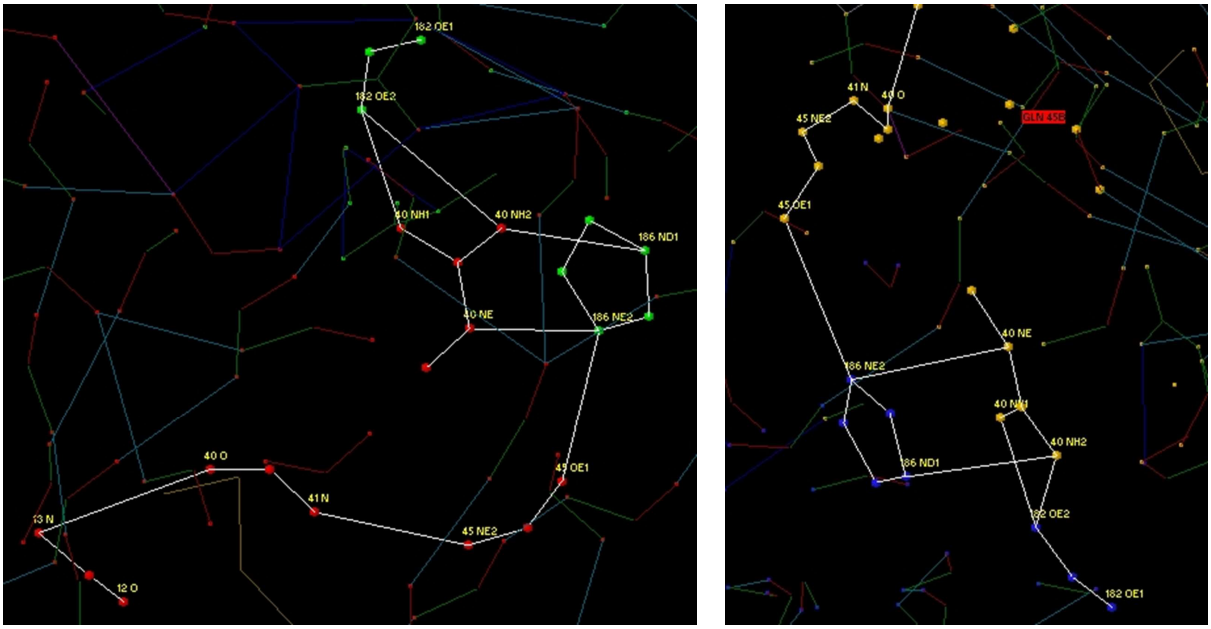

(**a**) (**b**)

Figure 4. Comparative analysis of CIHBS in complex between A (red) and C (green) subunits (**a**), complex between B (yellow) and D (blue) subunits (**b**).

Further analysis was made for Gln 175 of PSP and side chains Arg 25 and Gln 24 of LF, which form lengthy bonds inside LF. The structure for A–B and C–D was identical. Then analysis was completed for Arg 187 and Gln 183 of PSP and system of HN-C=O-groups of LF. For both cases, structures of CIHBS were identical. In the next step, in complex A–C, amino acids Glu 180, Gln 184 of PSP and Lys 39 of LF were analyzed, analogical amino acids were found in the B-D complex. Bonds were formed between Glu 171 of PSP and Gln 14 of LF. However, in this case, in the A–C complex, the bond spread through Thr 18 into the protein molecule. While in complex B–D, the bond was broken as a result of structural differences. Finally, a coupled hydrogen bond was formed between Glu 189 of PSP and Arg 54 of LF, which was identical for both complexes.

Figure 5 shows the structure of the PSP protein fragment for which the isolation of CIHBS was carried out. The names of the amino acids that are involved in the formation of CIHBS with LF are placed in white rectangles. It can be seen that almost all amino acids capable of forming H-bonds participate in the formation of the complex. The exceptions are Glu 170 and Lys 177. The latter forms an intramolecular CIHBS.

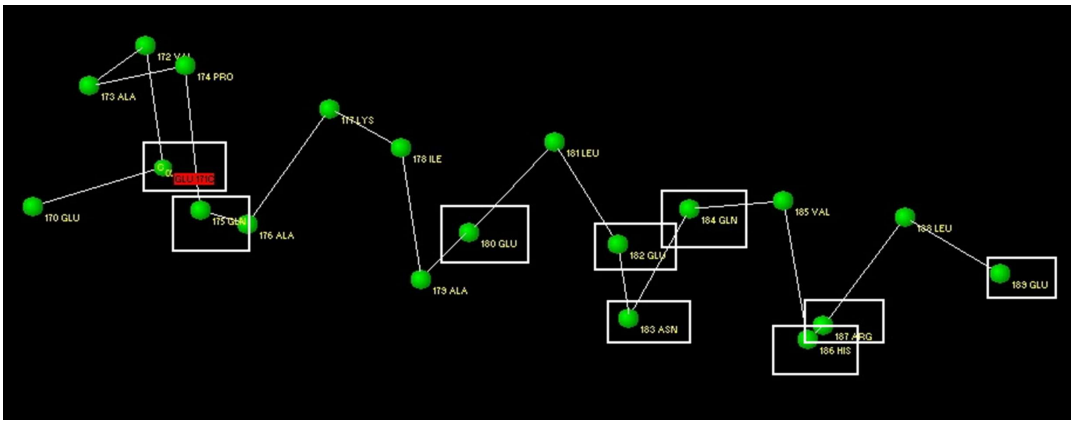

Figure 5. Fragment of PSP protein, forming a CIHBS link with N-lobe of LF.

The same amino acids are highlighted in bold on the proposed amino acid sequence to create a ligand for LG (Table 2). The peptide contains 40.91% of hydrophobic groups, 22.73% of neutral groups, 22.73% of acidic groups, and 13.64% of basic groups.

Table 2. The isolated fragment to form the ligand (peptide named LETI-11) to bind to lactoferrin.

170	**176**	**180**	**184**	**189**
GLU **GLU** VAL ALA PRO **GLN** ALA LYS ILE ALA **GLU** LEU **GLU** **ASN** **GLN** VAL **HIS** **ARG** LEU **GLU**				

3.2. Study of Peptide LETI-11 and Its Selective Binding of Lactoferrin

The peptide was studied with MS Voyager-DE BioSpectrometry Workstation (Applied Biosystems, Waltham, MA, USA) (Figure 6).

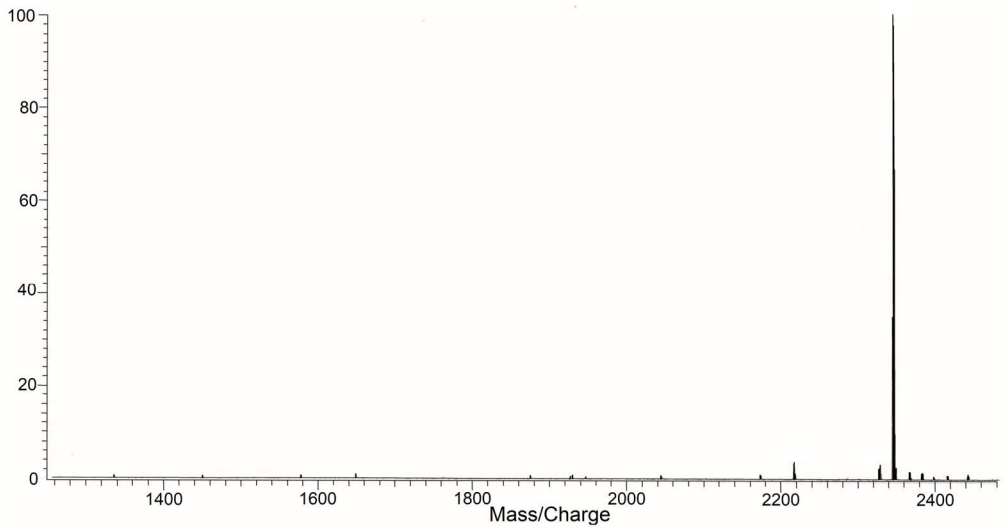

Figure 6. Mass-spectrometry data on the synthesized peptide LETI-11 (Mw = 2344.63); MS Voyager-DE BioSpectrometry Workstation (Applied Biosystems, Waltham, MA, USA).

The peptide LETI-11 was further analyzed by HPLC using chromatograph Gilson (France). The results of HPLC analysis are presented in Figure 7.

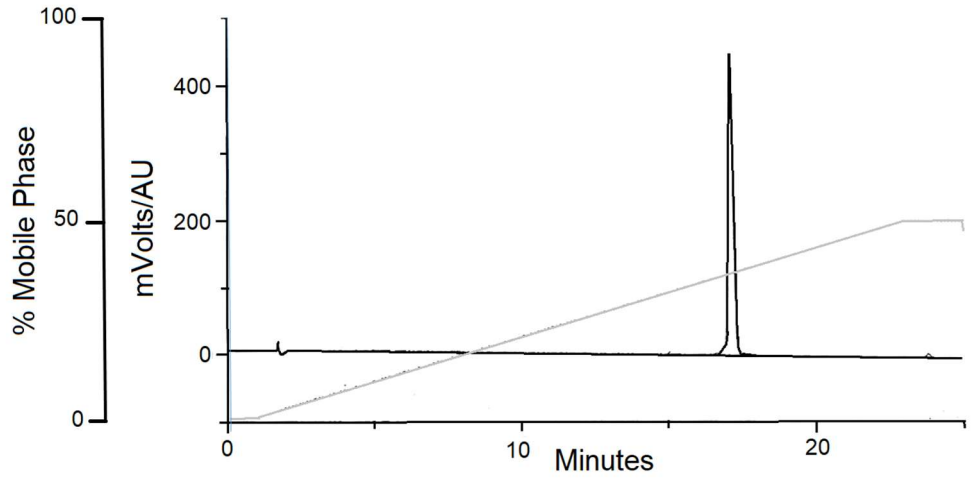

Figure 7. HPLC analysis of peptide LETI-11 sample. Column: DeltaPak C-18, 5 μm, 100 Å, 3.9 × 150 mm^2, gradient (0.1–50)% TFA in 20 min. Detector UV 220 nm.

The capillary electrophoresis system was used to study the interactions of peptide LETI-11 with target protein LF and two reference proteins—myeloperoxidase (MPO) and

myoglobin (MGB). At the first stage, the capillary system was calibrated with a series of peptide LETI-11 solutions of different concentrations within a range of 0.2–3.6 μM, using capillary prepared as procedure A. The electric field strength was 400 B.cm^{-1}. A sample electropherogram of LETI-11 of 3.6 μM concentration in Tris 0.01 M buffer pH 7.2 is presented in Figure 8a. The elution time was (5.2 ± 0.3) min. A relationship of zone areas at electropherograms versus sample concentration is presented in Figure 8b.

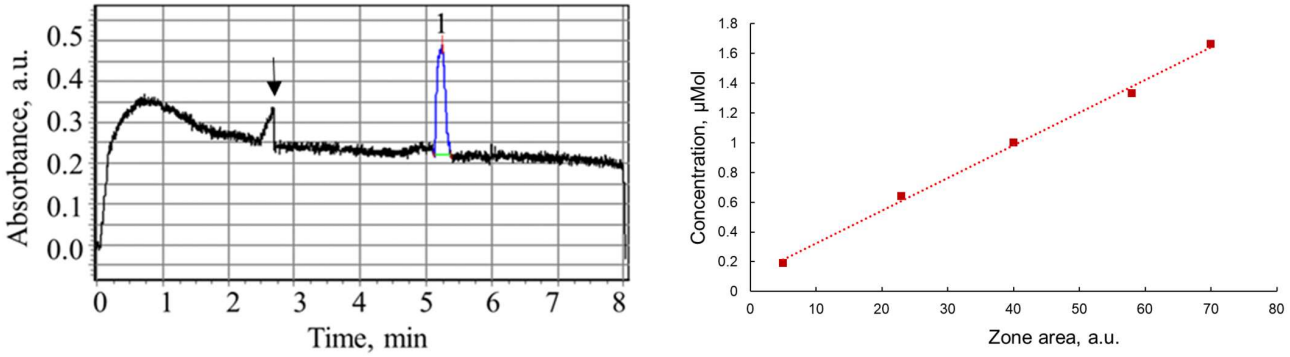

(**a**) (**b**)

Figure 8. Electropherogram of peptide LETI-11 (1), concentration 3.6 μM, Tris 0.01 M buffer pH 7.2, U = 20 kV, capillary length 50 cm, detection wavelength 200 nm. The leading peak reflects the system zone indicating the buffer velocity. Capillary treatment type A, the arrow shows the systemic peak corresponding to the electroosmotic flow velocity (**a**); relationship of LETI-11 zone areas, S (in arbitrary units) versus molar peptide LETI-11 concentrations (**b**).

Further experiments were carried out for LF (c = 3.6 μM) and the mixture of peptide LETI-11 and LF in the following molar ratios: 1:1; 1.5:1; 2:1; 2.5:1. The zone of LF did not appear in the detector area, due to the protein charge and polarity values that kept it stuck in the inlet volume (Figure 9a). The experiments of LF and LETI-11 mixtures demonstrated the split of the LETI-11 zone into 2 zones: 2 (5.2 ± 0.3 min) and 3 (7.8 ± 0.3 min), which could be attributed to the binding of LETI-11 to LF and subsequent reduction of the mobility of the complex compared to the LETI-11. Under selected conditions of CE, closer to physiological values in blood, the LF molecule is anionic and does not migrate, but after binding to a cationic peptide, the complex moves (Figure 9b).

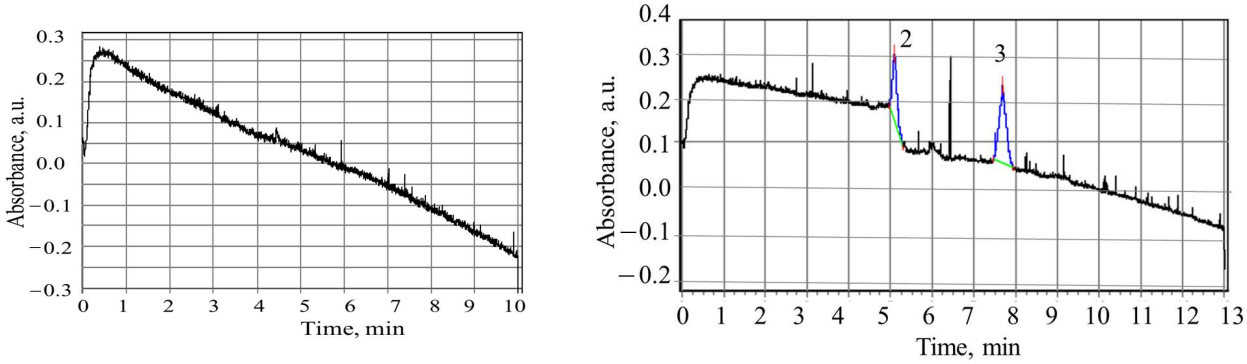

(**a**) (**b**)

Figure 9. Electropherograms of the LF (**a**) and the mixture of LETI-11 and LF at molar proportion of 1:1 (**b**). The conditions are as in Figure 8. Zone 2 (free LETI-11); zone 3 (complex of LETI-11 and LF). Capillary pretreatment type A.

The relationship of the zone areas presented in Figure 10 shows the inflection point at 1:1 molar concentration relationship of the components ($C_{LETI-11}$:C_{LF}), which is due to

the excess of peptide LETI-11 molar content over protein molar content, which remained constant. Figure 10 shows that the dependence of the area of the zone 2 (see Figure 8, i.e., the zone corresponding to the position of the LETI-11 zone without the addition of LF) versus content in mixture is linear. The dependence of the area of the zone 3 versus the molar ratio of the reaction components has a logarithmic character. This indicates the concentration dependence of the kinetics and equilibrium of the reaction. Based on the data obtained, it can be concluded that there is a statistical distribution of the reaction components and, as a result, a partial migration of LF molecules, and a partial capture of the peptide ligand by the protein.

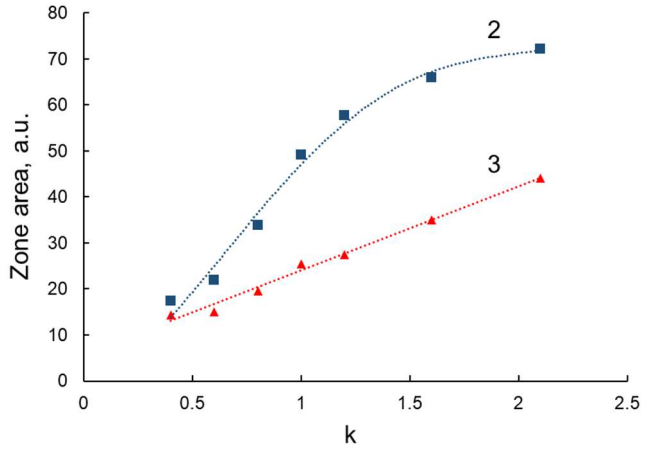

Figure 10. Relationship of sample areas of the split zones of LETI-11 (2) and complex of LETI-11 and LF (3) during electrophoresis under the presence of LF in solution, and the sum of the areas versus the ratio of components, k.

The reference experiments were performed with myeloperoxidase monomer (homoMPO) and myoglobin (MB). In Figure 11a, the electropherogram of LETI-11 and homoMPO is presented, showing the separate migration of the zones. In Figure 11b the electrophoregram of LETI-11 and myoglobin is presented, showing their separate migration.

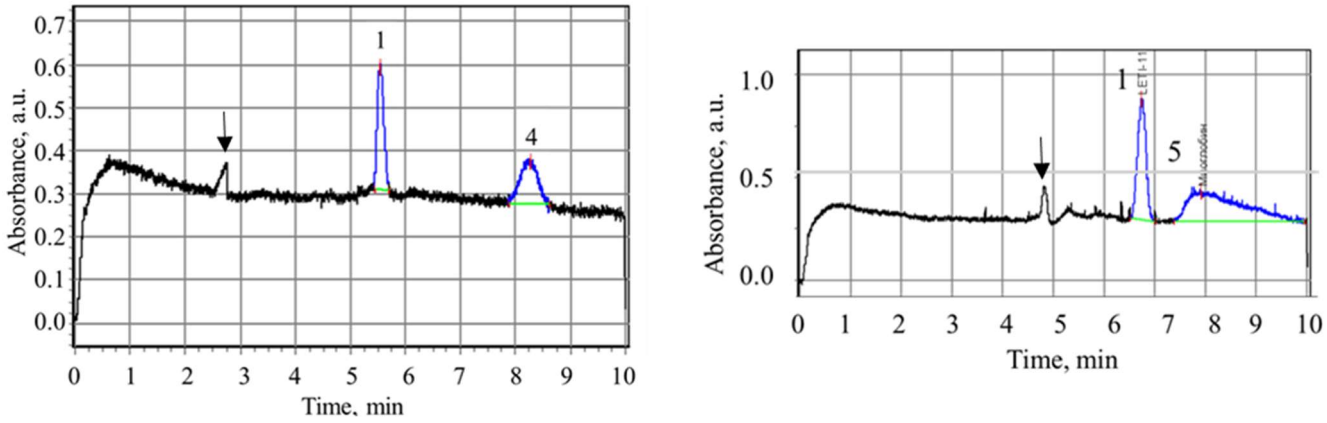

(**a**) (**b**)

Figure 11. Electropherogram of the mixture of (1) LETI-11 (1.5 μM), 5.5 min and (4) homoMPO (2.2 μM), 8.2 min, capillary pretreatment type A (**a**) and (1) LETI-11 (2.0 μM), 6.7 min and (5) MB (4.2 μM), 8 min, capillary pretreatment type B (**b**), pH = 7.2, 0.01 M tris-HCl buffer solution; the arrows show the systemic peak corresponding to the electroosmotic flow velocity.

The results demonstrate the lack of interaction between peptide LETI-11 and reference proteins MPO and MB, which manifested itself in separate migration of corresponding

zones. The range of concentrations investigated was: LETI-11 2.0 μM—MB (0.5–4.2 μM) and LETI-11 2.0 μM—MPO (0.5–2 μM).

Under conditions of type B preparation of capillary, which provide higher polarity of capillary wall, the higher migration times of all components were observed, and the transport effect for LF by LETI-11 has not been demonstrated.

As an additional test, we made a theoretical assessment of the peptide LETI-11 binding to human serum albumin (HAS), a protein present in the blood at a very high concentration. We performed molecular docking using the open-source service pepATTRACT [55,56], from which we selected the model of the complex of LETI-11 and HAS with the best docking score. Further, this model was transferred to the Protein 3D software, in which the absence of CIHBS was found at the site of the supposed docking contact, when in contrast they were observed in the case of lactoferrin.

4. Conclusions

In this work, the computer design of peptide architecture providing the complementary binding to lactoferrin (LF) for use in a biosensor system is presented. Modeling was carried out using the Protein 3D program and the natural architectonics of the interaction of LF and pneumococcal surface protein (PSP). The selection of the target protein was based on consideration that the formation of this complex is an example of the immune antimicrobial properties of LF [37]. The peptide sequence EEVAPQAQAKIAELENQVHRLE was proposed, which should demonstrate spatial complementarity to LF surface fragment. The peptide was synthesized and analyzed for purity and composition, which confirmed more than 95% purity. The interaction between LF and peptide (LETI-11) was studied using capillary electrophoresis at detection wavelength of 200 nm, where molar extinction coefficients of peptides are high. Cleavage of the LETI-11 peptide zone in the presence of LF in solution under mild conditions, close to physiological conditions, was observed. At the same time, no cleavage was observed in reference experiments with homomyeloperoxidase and myoglobin. The results indicate the interaction between LF and LETI-11.

Author Contributions: Conceptualization, T.Z., N.S., V.K. and V.L.; methodology, T.Z., N.S., V.K., A.K. (Alexey Kolobov), A.K. (Alexander Kolobov), Y.S., N.B. and V.L.; software, V.K.; validation, T.Z., N.S., A.K. (Alexander Kolobov), N.B. and Y.S.; formal analysis, N.B., Y.S. and V.L.; investigation, T.Z., N.S., V.K., A.K. (Alexey Kolobov), A.K. (Alexander Kolobov) and Y.S.; resources, T.Z., N.S., Y.S., A.K. (Alexey Kolobov), A.K. (Alexander Kolobov), N.B. and V.L.; data curation, T.Z. and V.K.; writing—original draft preparation, T.Z. and N.S.; writing—review and editing, T.Z. and N.S.; visualization, T.Z., N.S., V.K. and Y.S.; supervision, T.Z. and V.L.; project administration, T.Z. and V.L.; funding acquisition, T.Z. and N.S. All authors have read and agreed to the published version of the manuscript.

Funding: The reported study was funded by the Russian Science Foundation, project number 21-79-20219.

Institutional Review Board Statement: Not applicable.

Informed Consent Statement: Not applicable.

Data Availability Statement: Not applicable.

Acknowledgments: Authors acknowledge with thanks Sokolov V. A. from the Institute of Experimental Medicine, Russian Academy of Sciences, St. Petersburg for giving samples of proteins (homomyeloperoxydase and lactoferrin). The authors are also grateful to the Department of Mathematics and Natural Sciences of the Almazov National Medical Research Centre for providing equipment for capillary electrophoresis and to M.V. Baranova for carrying out the electrophoretic experiment.

Conflicts of Interest: The authors declare no conflict of interest.

References

1. Bhosale, S.D.; Moulder, R.; Venäläinen, M.S.; Koskinen, J.S.; Pitkänen, N.; Juonala, M.T.; Kähönen, M.A.P.; Lehtimäki, T.J.; Viikari, J.S.A.; Elo, L.L.; et al. Serum Proteomic Profiling to Identify Biomarkers of Premature Carotid Atherosclerosis. *Sci. Rep.* **2018**, *8*, 9209. [CrossRef] [PubMed]
2. Emilsson, V.; Gudmundsdottir, V.; Gudjonsson, A.; Jonmundsson, T.; Jonsson, B.G.; Karim, M.A.; Ilkov, M.; Staley, J.R.; Gudmundsson, E.F.; Launer, L.J.; et al. Coding and Regulatory Variants Are Associated with Serum Protein Levels and Disease. *Nat. Commun.* **2022**, *13*, 481. [CrossRef] [PubMed]
3. WHO. Noncommunicable Diseases. Key Facts. Available online: https://www.who.int/news-room/fact-sheets/detail/noncommunicable-diseases (accessed on 30 November 2022).
4. Sitkov, N.O.; Zimina, T.M.; Soloviev, A.V.; Lemozerskii, V.E.; Karasev, V.A. Development of Peptide Aptamers—3d Complementary Ligands for Selective Binding of Target Biomarkers of Diseases in Multiparametric Sensor Systems. In Proceedings of the 2019 IEEE Conference of Russian Young Researchers in Electrical and Electronic Engineering (EIConRus), St. Petersburg, Russia, 28–30 January 2019. [CrossRef]
5. Molvin, J.; Pareek, M.; Jujic, A.; Melander, O.; Råstam, L.; Lindblad, U.; Daka, B.; Leósdóttir, M.; Nilsson, P.M.; Olsen, M.H.; et al. Using a Targeted Proteomics Chip to Explore Pathophysiological Pathways for Incident Diabetes—The Malmö Preventive Project. *Sci. Rep.* **2019**, *9*, 272. [CrossRef] [PubMed]
6. Sitkov, N.; Zimina, T.; Kolobov, A.; Karasev, V.; Romanov, A.; Luchinin, V.; Kaplun, D. Toward Development of a Label-Free Detection Technique for Microfluidic Fluorometric Peptide-Based Biosensor Systems. *Micromachines* **2021**, *12*, 691. [CrossRef]
7. Neeli, I.; Radic, M. Current Challenges and Limitations in Antibody-Based Detection of Citrullinated Histones. *Front. Immunol.* **2016**, *7*, 528. [CrossRef] [PubMed]
8. Zhang, Y.; Lai, B.; Juhas, M. Recent Advances in Aptamer Discovery and Applications. *Molecules* **2019**, *24*, 941. [CrossRef]
9. Fathil, M.F.M.; Md Arshad, M.K.; Gopinath, S.C.B.; Hashim, U.; Adzhri, R.; Ayub, R.M.; Ruslinda, A.R.; Nuzaihan, M.N.M.; Azman, A.H.; Zaki, M.; et al. Diagnostics on Acute Myocardial Infarction: Cardiac Troponin Biomarkers. *Biosens. Bioelectron.* **2015**, *70*, 209–220. [CrossRef] [PubMed]
10. Ali, M.H.; Elsherbiny, M.E.; Emara, M. Updates on Aptamer Research. *Int. J. Mol. Sci.* **2019**, *20*, 2511. [CrossRef]
11. Li, J.; Tan, S.; Chen, X.; Zhang, C.-Y.; Zhang, Y. Peptide Aptamers with Biological and Therapeutic Applications. *Curr. Med. Chem.* **2011**, *18*, 4215–4222. [CrossRef]
12. Gold, L. SELEX: How It Happened and Where It Will Go. *J. Mol. Evol.* **2015**, *81*, 140–143. [CrossRef]
13. Dausse, E.; Barré, A.; Aimé, A.; Groppi, A.; Rico, A.; Ainali, C.; Salgado, G.; Palau, W.; Daguerre, E.; Nikolski, M.; et al. Aptamer Selection by Direct Microfluidic Recovery and Surface Plasmon Resonance Evaluation. *Biosens. Bioelectron.* **2016**, *80*, 418–425. [CrossRef]
14. Morris, G.M.; Lim-Wilby, M. Molecular Docking. *Mol. Modeling Proteins* **2008**, *443*, 365–382. [CrossRef]
15. Lensink, M.F.; Velankar, S.; Wodak, S.J. Modeling Protein-Protein and Protein-Peptide Complexes: CAPRI 6th Edition. *Proteins Struct. Funct. Bioinform.* **2016**, *85*, 359–377. [CrossRef]
16. Agrawal, P.; Singh, H.; Srivastava, H.K.; Singh, S.; Kishore, G.; Raghava, G.P.S. Benchmarking of Different Molecular Docking Methods for Protein-Peptide Docking. *BMC Bioinform.* **2019**, *19*, 105–124. [CrossRef]
17. Rhinehardt, K.L.; Mohan, R.V.; Srinivas, G. Computational Modeling of Peptide–Aptamer Binding. *Comput. Pept.* **2014**, 313–333. [CrossRef]
18. Karplus, M.; McCammon, J.A. Molecular Dynamics Simulations of Biomolecules. *Nat. Struct. Biol.* **2002**, *9*, 646–652. [CrossRef]
19. Senn, H.M.; Thiel, W. QM/MM Methods for Biomolecular Systems. *Angew. Chem. Int. Ed.* **2009**, *48*, 1198–1229. [CrossRef] [PubMed]
20. Karasev, V. A Model of Molecular Vector Machine of Proteins. *Biosystems* **2019**, *180*, 7–18. [CrossRef] [PubMed]
21. Visualizer of Supramolecular Biostructures «Protein 3d». Available online: http://protein-3d.ru/index_e.html (accessed on 30 November 2022).
22. Karasev, V.A.; Stefanov, V.E. Topological Nature of the Genetic Code. *J. Theor. Biol.* **2001**, *209*, 303–317. [CrossRef]
23. Pokrovskii, V.N. *The Mesoscopic Theory of Polymer Dynamics*; Springer: Dordrecht, The Netherlands, 2010. [CrossRef]
24. Karasev, V.A.; Luchinin, V.V.; Stefanov, V.E. Topological Coding: Towards New Materials for Molecular Electronics. *Adv. Funct. Mater.* **2002**, *12*, 461–469. [CrossRef]
25. Sitkov, N.O.; Zimina, T.M.; Karasev, V.A.; Lemozerskii, V.E.; Kolobov, A.A. Design of Peptide Ligands (Aptamers) for Determination of Myeloperoxidase Level in Blood Using Biochips. In Proceedings of the 2020 IEEE Conference of Russian Young Researchers in Electrical and Electronic Engineering (EIConRus), St. Petersburg, Russia, 27–30 January 2020. [CrossRef]
26. RCSB Protein Data. Available online: https://www.rcsb.org/ (accessed on 30 November 2022).
27. Misra, S.; Kumar, A.; Kumar, P.; Yadav, A.K.; Mohania, D.; Pandit, A.K.; Prasad, K.; Vibha, D. Blood-Based Protein Biomarkers for Stroke Differentiation: A Systematic Review. *PROTEOMICS—Clin. Appl.* **2017**, *11*, 1700007. [CrossRef] [PubMed]
28. Barro, C.; Zetterberg, H. The Blood Biomarkers Puzzle—A Review of Protein Biomarkers in Neurodegenerative Diseases. *J. Neurosci. Methods* **2021**, *361*, 109281. [CrossRef]
29. Ananthan, K.; Lyon, A.R. The Role of Biomarkers in Cardio-Oncology. *J. Cardiovasc. Transl. Res.* **2020**, *13*, 431–450. [CrossRef]

30. Sokolov, A.V.; Zakahrova, E.T.; Kostevich, V.A.; Samygina, V.R.; Vasilyev, V.B. Lactoferrin, Myeloperoxidase, and Ceruloplasmin: Complementary Gearwheels Cranking Physiological and Pathological Processes. *BioMetals* **2014**, *27*, 815–828. [CrossRef] [PubMed]
31. Lepanto, M.S.; Rosa, L.; Paesano, R.; Valenti, P.; Cutone, A. Lactoferrin in Aseptic and Septic Inflammation. *Molecules* **2019**, *24*, 1323. [CrossRef]
32. Kruzel, M.L.; Zimecki, M.; Actor, J.K. Lactoferrin in a Context of Inflammation-Induced Pathology. *Front. Immunol.* **2017**, *8*, 1438. [CrossRef]
33. Sokolov, A.V.; Dubrovskaya, N.M.; Kostevich, V.A.; Vasilev, D.S.; Voynova, I.V.; Zakharova, E.T.; Runova, O.L.; Semak, I.V.; Budevich, A.I.; Nalivaeva, N.N.; et al. Lactoferrin Induces Erythropoietin Synthesis and Rescues Cognitive Functions in the Offspring of Rats Subjected to Prenatal Hypoxia. *Nutrients* **2022**, *14*, 1399. [CrossRef] [PubMed]
34. Skarżyńska, E.; Żytyńska-Daniluk, J.; Lisowska-Myjak, B. Correlations between Ceruloplasmin, Lactoferrin and Myeloperoxidase in Meconium. *J. Trace Elem. Med. Biol.* **2017**, *43*, 58–62. [CrossRef]
35. Grudinin, N.V.; Karev, V.E.; Bunenkov, N.S.; Komok, V.V.; Kostevitch, V.V.; Gorbunov, N.P.; Sokolov, A.V.; Karpov, A.A.; Lepik, K.V.; Shvetsov, A.N.; et al. Histological features and blood plasma changes after heterotopic heart transplantation. *Cell. Ther. Transplant.* **2018**, *7*, 59–60.
36. Zhang, Y.; Lu, C.; Zhang, J. Lactoferrin and Its Detection Methods: A Review. *Nutrients* **2021**, *13*, 2492. [CrossRef] [PubMed]
37. Monnard, C.; Vernet, M. Détermination de la lactoferrine plasmatique par une méthode immunoenzymatique "double sandwich" en phase hétérogène [Determination of plasma lactoferrin by the "double sandwich" immunoenzymatic method in heterogeneous phase]. *Pathol. -Biol.* **1988**, *36*, 941–944. [PubMed]
38. Mantel, C.; Miyazawa, K.; Broxmeyer, H.E. Physical Characteristics and Polymerization During Iron Saturation of Lactoferrin, A Myelopoietic Regulatory Molecule With Suppressor Activity. *Adv. Exp. Med. Biol.* **1994**, 121–132. [CrossRef]
39. Bagby, G.J.; Bennett, R. Feedback Regulation of Granulopoiesis: Polymerization of Lactoferrin Abrogates Its Ability to Inhibit CSA Production. *Blood* **1982**, *60*, 108–112. [CrossRef] [PubMed]
40. Sitkov, N.; Zimina, T.; Kolobov, A.; Sevostyanov, E.; Trushlyakova, V.; Luchinin, V.; Krasichkov, A.; Markelov, O.; Galagudza, M.; Kaplun, D. Study of the Fabrication Technology of Hybrid Microfluidic Biochips for Label-Free Detection of Proteins. *Micromachines* **2021**, *13*, 20. [CrossRef] [PubMed]
41. Jaradat, D.M. Thirteen Decades of Peptide Synthesis: Key Developments in Solid Phase Peptide Synthesis and Amide Bond Formation Utilized in Peptide Ligation. *Amino Acids* **2017**, *50*, 39–68. [CrossRef] [PubMed]
42. Zaia, J.; Annan, R.S.; Biemann, K. The Correct Molecular Weight of Myoglobin, a Common Calibrant for Mass Spectrometry. *Rapid Commun. Mass Spectrom.* **1992**, *6*, 32–36. [CrossRef]
43. Myoglobin from Equine Heart. Available online: https://www.sigmaaldrich.com/RU/en/product/sigma/m9267 (accessed on 30 November 2022).
44. Davies, M.J. Myeloperoxidase-Derived Oxidation: Mechanisms of Biological Damage and Its Prevention. *J. Clin. Biochem. Nutr.* **2010**, *48*, 8–19. [CrossRef]
45. Malle, E.; Furtmüller, P.G.; Sattler, W.; Obinger, C. Myeloperoxidase: A Target for New Drug Development? *Br. J. Pharmacol.* **2007**, *152*, 838–854. [CrossRef]
46. Mathy-Hartert, M.; Bourgeois, E.; Grülke, S.; Deby-Dupont, G.; Caudron, I.; Deby, C.; Lamy, M.; Serteyn, D. Purification of myeloperoxidase from equine polymorphonuclear leucocytes. *Can. J. Vet. Res.* **1998**, *62*, 127. [PubMed]
47. Li, J.; Ding, X.; Chen, Y.; Song, B.; Zhao, S.; Wang, Z. Determination of Bovine Lactoferrin in Infant Formula by Capillary Electrophoresis with Ultraviolet Detection. *J. Chromatogr. A* **2012**, *1244*, 178–183. [CrossRef]
48. Shimazaki, K.-I.; Kawaguchi, A.; Sato, T.; Ueda, Y.; Tomimura, T.; Shimamura, S. Analysis of Human and Bovine Milk Lactoferrins by Rotofor and Chromatofocusing. *Int. J. Biochem.* **1993**, *25*, 1653–1658. [CrossRef]
49. Senkovich, O.; Cook, W.J.; Mirza, S.; Hollingshead, S.K.; Protasevich, I.I.; Briles, D.E.; Chattopadhyay, D. Structure of a Complex of Human Lactoferrin N-Lobe with Pneumococcal Surface Protein A Provides Insight into Microbial Defense Mechanism. *J. Mol. Biol.* **2007**, *370*, 701–713. [CrossRef]
50. Isoelectric Point Calculator. Available online: https://www.bachem.com/knowledge-center/peptide-calculator/ (accessed on 30 November 2022).
51. Andreeva, A.; Budenkova, E.; Babich, O.; Sukhikh, S.; Ulrikh, E.; Ivanova, S.; Prosekov, A.; Dolganyuk, V. Production, Purification, and Study of the Amino Acid Composition of Microalgae Proteins. *Molecules* **2021**, *26*, 2767. [CrossRef] [PubMed]
52. Gill, S.C.; von Hippel, P.H. Calculation of Protein Extinction Coefficients from Amino Acid Sequence Data. *Anal. Biochem.* **1989**, *182*, 319–326. [CrossRef] [PubMed]
53. Saraiva, M.A. Interpretation of α-Synuclein UV Absorption Spectra in the Peptide Bond and the Aromatic Regions. *J. Photochem. Photobiol. B Biol.* **2020**, *212*, 112022. [CrossRef] [PubMed]
54. Sun, X.-L.; Baker, H.M.; Shewry, S.C.; Jameson, G.B.; Baker, E.N. Structure of Recombinant Human Lactoferrin Expressed in Aspergillus Awamori. *Acta Crystallogr. Sect. D Biol. Crystallogr.* **1999**, *55*, 403–407. [CrossRef] [PubMed]

55. Schindler, C.E.M.; de Vries, S.J.; Zacharias, M. Fully Blind Peptide-Protein Docking with PepATTRACT. *Structure* **2015**, *23*, 1507–1515. [CrossRef]
56. De Vries, S.J.; Rey, J.; Schindler, C.E.M.; Zacharias, M.; Tuffery, P. The PepATTRACT Web Server for Blind, Large-Scale Peptide–Protein Docking. *Nucleic Acids Res.* **2017**, *45*, W361–W364. [CrossRef]